Three-Dimensional Kinematic Modelling of the Human Shoulder Complex—Part I: Physical Model and Determination of Joint Sinus Cones

A. E. Engin
Professor,
Department of Engineering Mechanics,
The Ohio State University,
Columbus, Ohio, 43210
Mem. ASME

S. T. Tümer
Assistant Professor,
Mechanical Engineering Department,
King Saud University,
Riyadh 11421, Saudi Arabia

Modelling of the human shoulder complex is essential for the multi-segmented mathematical models as well as design of the shoulder mechanism of anthropometric dummies. In Part I of this paper a three-dimensional kinematic model is proposed by utilizing the concepts of kinematic links, joints, and joint sinuses. By assigning appropriate coordinate systems, parameters required for complete quantitative description of the proposed model are identified. The statistical in-vivo data base established by Engin and Chen (1986) is cast in a form compatible with the model by obtaining a set of unit vectors describing circumductory motion of the upper arm in a torso-fixed coordinate system. This set of unit vectors is then employed in determining the parameters of a composite shoulder complex sinus of a simplified version of the proposed model. Two methods, namely the flexible tolerance and the direct methods, are formulated and tested for the determination of an elliptical cone surface for a given set of generating unit vectors. Numerical results are presented for the apex angles and orientation of the composite joint sinus cone with respect to the anatomical directions.

Introduction

The proper biomechanical description and simulation of the human shoulder complex is not only needed for a successful multi-segmented mathematical modelling of the total human body, but also is essential in designing a human shoulder mechanism to be used as a part of an anthropometric dummy. Furthermore, the human shoulder complex models provide means to identify risk factors in the treatment of degenerative shoulder lesions. The term "shoulder complex" refers to the combination of the shoulder joint (the glenohumeral joint) and the shoulder girdle which includes the clavicle and scapula and their articulations. Thus, the usage of the term shoulder joint is somewhat misleading if one does not bear in mind the various components of the region and their interactions. The research and studies on the shoulder complex has more than a century long history, and a brief summary of the subject matter prior to 1980 is provided by Engin (1980).

Biomechanical models of the human should complex range from a qualitative planar kinematic model (Dvir and Berme, 1978) to that of Högfors et al. (1987) that aims at prediction of muscle forces in the shoulder region as functions of arm position and external load in static and quasistatic situations in three dimensions. The success of biomechanical modelling of the shoulder complex is generally hindered by the lack of appropriate data base as well as the anatomical complexity of the region. Recently, Engin and Chen (1986a) have established a statistical in-vivo data base for the shoulder complex sinus of male population of ages 18–32. They expressed the numerical results in functional expansion form relative to a locally defined joint axis system. Engin and Chen (1986b) have also determined the three-dimensional passive resistive joint properties beyond the maximal voluntary shoulder complex sinus.

In this two-part paper, the statistical data base established by Engin and Chen (1986a) will be utilized in developing a three-dimensional kinematic model of the human shoulder complex. In Part I, a physical model, which consists of an open loop chain of four links connected to each other by universal and sleeve joints, is proposed for the human shoulder complex. In order to describe the proposed mechanism quantitatively, the statistical database of Engin and Chen (1986a) is then converted from a format of single-valued functional relationship, expressed in a local joint axis system, into a set of direction cosines for the humerus in a torso-fixed coordinate system. Since the main theme of the proposed mechanism is the establishment of individual joint sinus cones, Part I also contains mathematical procedure of obtaining these cones from a set of direction cosines.

Contributed by the Bioengineering Division for publication in the JOURNAL OF BIOMECHANICAL ENGINEERING. Manuscript received in final form by the Bioengineering Division June 9, 1988.

Downloaded From: https://biomechanical.asmedigitalcollection.asme.org on 06/29/2019 Terms of Use: http://www.asme.org/about-asme/terms-of-use

Copyright © 1989 by ASME

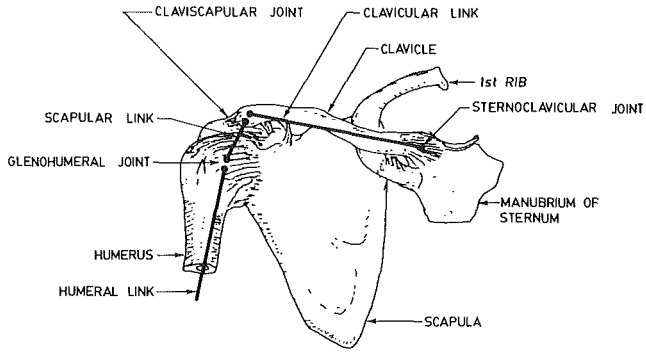

Fig. 1 Principal bones and joints of the shoulder complex. The heavy lines designate the clavicular, scapular, and humeral links

Proposed Shoulder Mechanism (Physical Model)

The most striking feature of the shoulder complex is the presence of independent articulations among the bones of the shoulder complex, i.e., the clavicle, scapula, humerus, and the thorax as depicted in Fig. 1. The sternoclavicular and the claviscapular joints are the two articulations of the clavicle. The glenohumeral joint is a partial ball and socket joint where the humerus articulates with the glenoid cavity of the scapula. The motion of the scapula with respect to torso is sometimes defined as the forth articulation and named as the scapulothoracic joint. However, in the true sense, the scapulothoracic articulation is not a joint; but this definition is of some value when describing the movements of the scapula over the thorax. Brief anatomical and kinesiological descriptions of these joints are previously given (Engin, 1980), and more detailed descriptions can be found in Steindler (1955) or *Gray's Anatomy* (1973).

Dempster (1965), in his studies on the range-of-movement of shoulder cadaveric specimens, introduced the concept of links to explain the relative motions of clavicle, scapula, and humerus. A link is defined as a straight line between two neighboring articulating joints. Thus, the clavicular link is a straight line between the sternoclavicular joint and the claviscapular joint; the scapular link is a line from the claviscapular joint to the average center of curvature for the humeral articular face; and the humeral link is a line between the average center of the humeral head and the average center of curvature of the capitulum at the elbow joint. In Fig. 1 these three links are shown by heavy lines.

Since the terms *joint sinus* and *joint sinus cone* are extensively used in this paper, let us define these two terms. *Joint sinus* is the total range of angular motion permitted by a moving link of a joint when the other link is rigidly fixed. *The joint sinus cone* is the conical surface enveloping the joint sinus and having its apex at the functional center of the joint. Thus, in view of Fig. 1, three individual joint sinus cones, namely, sternoclavicular, claviscapular, and glenohumeral cones can be defined. More specifically, the sternoclavicular cone represents the joint sinus of the clavicular link with respect to the thorax, the claviscapular cone represents the joint sinus of the scapular link with respect to the clavicle, and finally the glenohumeral cone represents the joint sinus of the humeral link with respect to the scapula. It is also possible to define a composite "shoulder complex sinus cone" describing the total range of angular motion permitted by the upper arm (humeral link) with respect to the torso.

Based on aforementioned concepts a linkage mechanism depicted in Fig. 2 is proposed for kinematic representation of the shoulder complex. Basic components of this mechanism are links, single degree-of-freedom sleeve joints, and two degrees-of-freedom universal joints that are composed of two single degree-of-freedom revolute joints along two intersecting

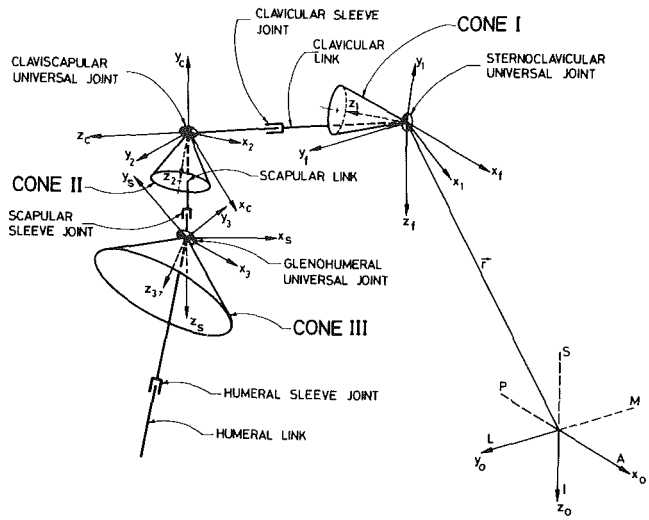

Fig. 2 Schematic representation of the proposed shoulder complex model

perpendicular axes. Besides these components, universal joint stops or templetes representing individual joint sinus cones and appropriate mechanical stops for limiting the sleeve rotations are added. The shape of these cones was shown to be approximately elliptical by Dempster (1965) according to his tests on cadaveric specimens. The universal joints allow the links to rotate with respect to each other, whereas the sleeve joints provide rotational freedom about individual link axes. It should be noted that combined effect of universal joint and a sleeve joint is one of a ball and socket.

Several coordinate systems need to be defined for the quantitative description of the proposed shoulder mechanism, Fig. 2. The origin of the torso-fixed right-handed orthogonal coordinate system (x_0, y_0, z_0) is defined by establishing three orthogonal planes in the following manner. The first plane (the sagittal plane), x_0z_0, is established by three bony landmarks (suprasternale, cervicale, and mid-spine at the level of the tenth rib); the second plane (the frontal plane), y_0z_0, that is perpendicular to the first one is established by two landmarks (cervicale and mid-spine at the level of the tenth rib), the third plane (the transverse plane), x_0y_0, which is perpendicular to both x_0z_0 and y_0z_0 is established by a single landmark (mid-spine at the level of the tenth rib). In this way, x_0, y_0 and z_0 axes are, respectively, aligned along the anatomical directions anterior-posterior (A-P) toward anterior (A), medial-lateral (M-P) toward lateral (L), and superior-inferior (S-I) toward inferior (I). The body-fixed coordinate system (x_f, y_f, z_f) may be considered as the reference system attached to the frame (fixed link) of the shoulder complex mechanism. It is obtained by translating the torso-fixed system to the sternoclavicular joint center by the vector **r**. The two moving coordinate systems (x_c, y_c, z_c) and (x_s, y_s, z_s) are attached to the distal ends of the clavicular and scapular links, respectively, in such a way that if one imagines a fictitious orientation of clavicular and scapular links becoming collinear and running along inferior direction ($+z_0$-axis), the moving coordinate systems take a parallel configuration with the torso-fixed system. The sternoclavicular joint sinus cone (Cone I) is fixed to the frame (torso) at the sternoclavicular joint center, and its orientation is defined by the (x_1, y_1, z_1) coordinate system in such a manner that z_1 is along the cone axis, and x_1 and y_1 are parallel to the major and minor axes of elliptical cross section of the cone. The transformation between the body-fixed (x_f, y_f, z_f) and Cone I-fixed (x_1, y_1, z_1) systems is one of rotation and can conveniently be described by three Euler angles, α_1, β_1, and γ_1 for which the associated convention will be defined later. The

Downloaded From: https://biomechanical.asmedigitalcollection.asme.org on 06/29/2019 Terms of Use: http://www.asme.org/about-asme/terms-of-use

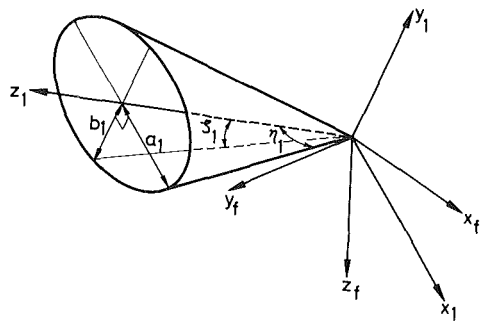

Fig. 3 Half apex angles and semi-axes of the joint sinus cone

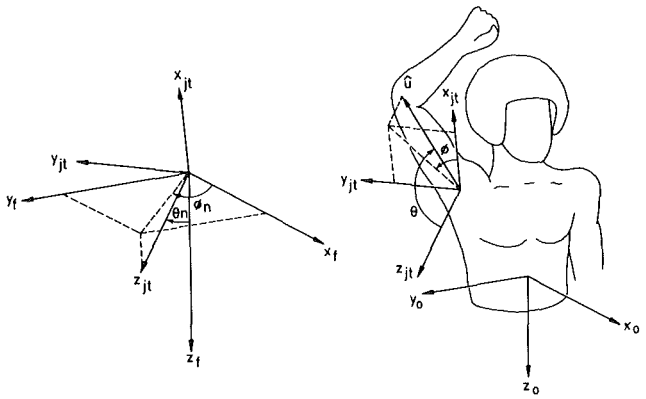

Fig. 4 Relative orientation of the body-fixed (x_f, y_f, z_f) and joint axis (x_{jt}, y_{jt}, z_{jt}) systems, and the spherical angles, ϕ and θ, defining humerus orientation (after Engin and Chen, 1986a)

size of Cone I, on the other hand, can be defined by the two half apex angles η_1 andζ_1 as shown in Fig. 3. Thus, Cone I is fully defined by five parameters, namely α_1, β_1, γ_1, η_1, and ζ_1. The claviscapular joint sinus cone (Cone II) is fixed to the clavicle at the claviscapular joint center, and its orientation is defined by the (x_2, y_2, z_2) coordinate system in the same manner as that of Cone I. Five parameters defining Cone II with respect to clavicle are α_2, β_2, γ_2, η_2, and ζ_2, where α_2, β_2, and γ_2 are the Euler angles for the transformation between the clavicle-fixed (x_c, y_c, z_c) and Cone II-fixed (x_2, y_2, z_2) coordinate systems, and η_2 and ζ_2 are the half apex angles. Likewise, the glenohumeral joint sinus cone (Cone III) is defined with respect to the scapula by a third set of five parameters i.e., α_3, β_3, γ_3, η_3, and ζ_3. Note that in this case, the Euler angles γ_3, β_3, and γ_3 refer to the transformation between the scapula-fixed (x_s, y_s, z_s) and Cone III-fixed (x_3, y_3, z_3) coordinate systems. It is important to point out at this stage that in addition to the aforementioned 15 cone parameters, one has to specify 12 more parameters to be able to utilize the shoulder-upper arm model either in a multi-segmented mathematical model of the human body or as a part of an anthropometric dummy. These additional parameters are the 3 components of vector **r**, Fig. 2, required for placement of the sternoclavicular joint with respect to torso, the clavicular, scapular and humeral link lengths, and finally 6 limiting values for the sleeve rotations of the three links in both directions from their respective nominal positions. Note that the first 6 of the 12 additional parameters are available from anthropometric measurements (e.g., Dempster, 1965). In Part II of this paper, we will present a method of determining all remaining parameters except the limiting values for the sleeve rotations of the humeral link (i.e., a total of 19 parameters) via an optimization scheme.

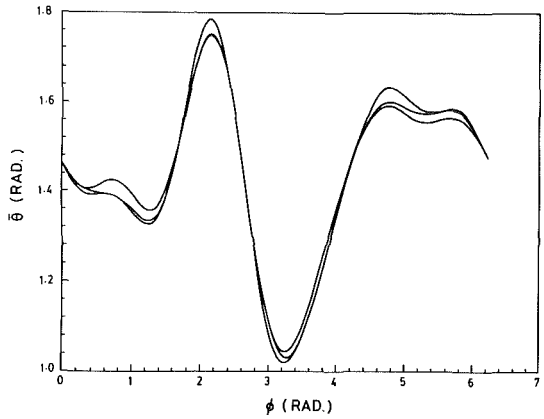

Fig. 5 $\bar{\theta}(\phi)$ for three different runs for all subjects (after Engin and Chen, 1986a)

Utilization of Available Database

Dempster (1965) has collected a limited amount of data on specially prepared cadaveric specimens which can be used to estimate the values of several aforesaid parameters of the proposed model. Apart from being incomplete, since the data obtained by Dempster (1965) are based on in-vitro measurments they may not be considered as indicative of in-vivo conditions. As mentioned earlier, Engin and Chen (1986a) were the first to provide statistically meaningful in-vivo data base for the kinematics of the shoulder complex. Their data collection methodology, which utilizes sonic emitters and data analysis technique based on selection of the "most accurate" data set, had been previously developed (Engin et al., 1984), and applied to provide passive resistive properties of the human shoulder complex for *one* subject (Engin and Peindl, 1985). Engin and Chen (1986a) have applied the research program described in (Engin and Peindl, 1985), and have statistically analyzed the data collected for *ten* male subjects of ages 18 through 32 possessing neither musculoskeletal abnormalities nor any history of trauma in the shoulder complex region. The subjects were instructed to move their arms along the maximal voluntary range of circumductory type of motion, and 3-D coordinates of a distal point on the humerus (a specific point on the elbow) were monitored in the same torso-fixed coordinate system (x_0, y_0, z_0) defined earlier. In order to be able to express the orientation of the upper arm in a single-valued functional relationship a local joint axis system (x_{jt}, y_{jt}, z_{jt}) was established by following a unique procedure. This local joint axis system is specified by two spherical angles ϕ_n and θ_n as shown in Fig. 4 reproduced from Engin and Chen (1986a). Sample mean $\bar{\phi}_n$ and $\bar{\theta}_n$ for three test runs of ten subjects were calculated as 58.65 and 78.48 deg, respectively. Thus, the orientation of the upper arm can now be defined by means of the spherical coordinates ϕ and θ measured in the local joint axis system in a single-valued functional relationship, i.e., $\theta=\theta(\phi)$. The sample means of all subjects $\bar{\theta}=\bar{\theta}(\phi)$ are reproduced in Fig. 5 for three different runs. Any point of $\bar{\theta}=\bar{\theta}(\phi)$ represents a particular orientation of the upper arm in local joint axis system. However, what is needed for the proposed shoulder complex model is the expression of the same in the torso-fixed (or the parallel body-fixed) coordinate system. Let $\hat{u}$ be a unit vector describing upper arm orientation, Fig. 4. This unit vector is represented in local joint axis and body-fixed systems by $\hat{u}_{jt}$ and $\hat{u}_f$, respectively. It is clear from Fig. 4 that

$$\hat{u}_{jt}=[x_{jt}y_{jt}z_{jt}]^T=[S\bar{\theta}C\phi \quad S\bar{\theta}S\phi \quad C\bar{\theta}]^T \tag{1}$$

where S and C stand for sine and cosine functions, respectively. The local joint axis system (x_{jt}, y_{jt}, z_{jt}) is obtained from the body-fixed system (x_f, y_f, z_f) by first rotating an angle $\bar{\phi}_n$

Downloaded From: https://biomechanical.asmedigitalcollection.asme.org on 06/29/2019 Terms of Use: http://www.asme.org/about-asme/terms-of-use

about z_f axis, then rotating the intermediate axis system by an angle $\bar{\theta}_n$ about intermediate y_f axis, as implied in Fig. 4. By utilizing elementary transformation matrices in the prescribed order we can then get

$$\hat{u}_f = [x_f y_f z_f]^T = [M]\hat{u}_{jt} \tag{2}$$

where

$$[M] = \begin{bmatrix} C\bar{\theta}_n C\bar{\phi}_n & -S\bar{\phi}_n & S\bar{\theta}_n C\bar{\phi}_n \\ C\bar{\theta}_n S\bar{\phi}_n & C\bar{\phi}_n & S\bar{\theta}_n S\bar{\phi}_n \\ -S\bar{\theta}_n & 0 & C\bar{\theta}_n \end{bmatrix} \tag{3}$$

The set of $\hat{u}_f$ unit vectors now available can be utilized to quantitatively determine the composite shoulder complex sinus cone which was previously defined. This composite cone represents the combined effects of all three joints of the shoulder complex, and leads us to a simplified version of the proposed mechanism as shown in Fig. 6. In this mechanism only the motion of humerus is considered with respect to torso; however, the motions of clavicular and scapular links are inherently present since the composite cone covers the motions of all the links. Clearly, the position $\mathbf{r}'$, of the single universal joint does not correspond to a particular joint. The method of determining the vector $\mathbf{r}'$ from the 3-D coordinate data of a distal point on the humerus during circumductory motion of the upper arm is reported elsewhere (Engin and Tümer, 1987). The following section describes the method by which the set of $\hat{u}_f$ unit vectors are utilized to define the elliptical cone for the composite sinus of the simplified mechanism. The same method will also be used later on in Part II of this paper for the quantitative determination of the individual joint sinus cones of the initially proposed shoulder complex mechanism.

Determination of the Composite Sinus Cone

Consider Fig. 6, which shows the composite sinus cone. Let $O'C$ be unity, so that the half apex angles of the cone, η_t and ζ_t are related to the lengths a_t and b_t of the semi-axes of elliptic cross section at C, by

$$a_t = \tan \eta_t, \quad b_t = \tan\zeta_t \tag{4}$$

Let $\hat{u}$ be a unit vector lying on the generating surface of the cone, represented by $\hat{u}_f = [x_f\, y_f\, z_f]^T$ in body-fixed, and $\hat{u}_t = [x_t\, y_t\, z_t]^T$ in cone-fixed systems. Knowing the parametric equation of the elliptical cone in the cone-fixed system, the following relation can be written between the components of $\hat{u}_t$:

$$\left(\frac{x_t}{a_t}\right)^2 + \left(\frac{y_t}{b_t}\right)^2 = z_t^2 \tag{5}$$

The transformation between $\hat{u}_t$ and $\hat{u}_f$ can be accomplished by three Euler angles α_t, β_t, and γ_t according to the rotation sequence shown in Fig. 7, and the resulting transformation matrix $[R]_{ft}$ is given by

$$[R]_{ft} = \begin{bmatrix} r_{11} & r_{12} & r_{13} \\ r_{21} & r_{22} & r_{23} \\ r_{31} & r_{32} & r_{33} \end{bmatrix}$$

$$= \begin{bmatrix} C\beta_t C\gamma_t & -C\beta_t S\gamma_t & S\beta_t \\ S\alpha_t S\beta_t C\gamma_t + C\alpha_t S\gamma_t & -S\alpha_t S\beta_t S\gamma_t + C\alpha_t C\gamma_t & -S\alpha_t C\beta_t \\ -C\alpha_t S\beta_t C\gamma_t + S\alpha_t S\gamma_t & C\alpha_t S\beta_t S\gamma_t + S\alpha_t C\gamma_t & C\alpha_t C\beta_t \end{bmatrix} \tag{6}$$

Therefore

$$\hat{u}_t = [R]_{ft}^T \hat{u}_f \tag{7}$$

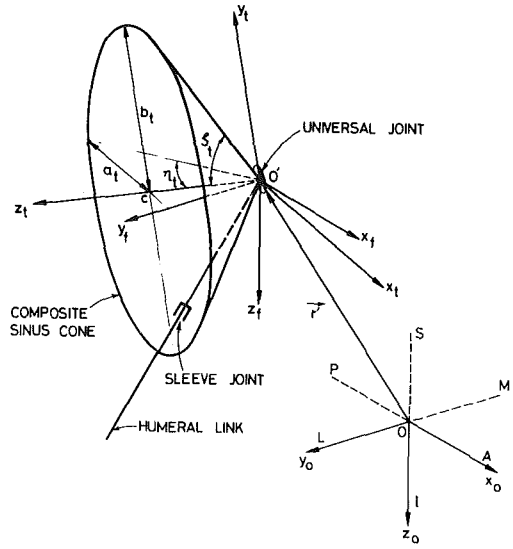

Fig. 6 Simplified version of the proposed shoulder complex model: composite joint sinus cone

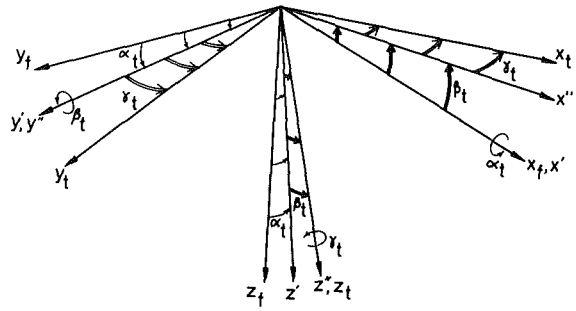

Fig. 7 Cone-fixed (x_t, y_t, z_t) system obtained by successive rotations α_t, β_t, and γ_t from the body-fixed (x_f, y_f, z_f) system

We next pick 32 equally spaced points from Fig. 5 within interval $0 \le \phi \le 2\pi$. The $\hat{u}_f$ vectors corresponding to these 32 data points are calculated from equations (1) thru (3). At this point the results were checked by noting that for the unit vector $\hat{u}_f = [x_f\, y_f\, z_f]^T$, the equation of $x_f^2 + y_f^2 + z_f^2 = 1$ is satisfied to the fifth decimal point accuracy.

The problem is now one of finding the parameters of the elliptical cone (α_t, β_t, γ_t, a_t, b_t) from equations (5) thru (7) for 32 sets of $\hat{u}_f$ available. The redundant data permits an optimization scheme to be used to find the best-fitted elliptical cone surface in the least squares sense. For a typical ith unit vector on the cone surface, $\hat{u}_f{}^i = [x_f{}^i\, y_f{}^i\, z_f{}^i]^T$, the following relation can be written from equations (5) thru (7):

$$t_i(\alpha_t,\beta_t,\gamma_t,a_t,b_t) = \frac{1}{a_t^2}(r_{11}x_f^i + r_{21}y_f^i + r_{31}z_f^i)^2 + \frac{1}{b_t^2}(r_{12}x_f^i + r_{22}y_f^i + r_{32}z_f^i)^2 - (r_{13}x_f^i + r_{23}y_f^i + r_{33}z_f^i)^2 = 0 \quad i = 1, \ldots, n \tag{8}$$

where r_{kl} are given by equation (6), and $n = 32$. Clearly for

Downloaded From: https://biomechanical.asmedigitalcollection.asme.org on 06/29/2019 Terms of Use: http://www.asme.org/about-asme/terms-of-use

$n>5$ there is no solution for equation (8), but for fixed α_t, β_t, γ_t, a_t, b_t we can evaluate t_i as:

$$t_i(\alpha_t, \beta_t, \gamma_t, a_t, b_t) = \epsilon_i \tag{9}$$

Then, the problem of finding the best-fitted cone in the least squares sense can be formulated as the following optimization problem: Find the parameter values α_t, β_t, γ_t, a_t, and b_t such that

$$\Phi(\alpha_t,\beta_t,\gamma_t,a_t,b_t) = \frac{1}{2}\sum_1^n \epsilon_i^2 \tag{10}$$

is a minimum. This is a highly nonlinear optimization problem and requires numerical solution. It is a well-known fact that the numerical solution to such problems can not be relied upon unless they are checked for accuracy and stability. For this reason a change of variables is performed and an alternative form of equation (8) is obtained

$$\begin{aligned} t_i(\alpha_t,\beta_t,\gamma_t,a_t,b_t) &= A_t(r_{11}x_f^i + r_{21}y_f^i + r_{31}z_f^i)^2 \\ &\quad + B_t(r_{12}x_f^i + r_{22}y_f^i + r_{32}z_f^i)^2 \\ &\quad - (r_{13}x_f^i + r_{23}y_f^i + r_{33}z_f^i)^2 = 0 \quad i=1, \ldots, n \end{aligned} \tag{11}$$

where $A_t = 1/a_t^2$ and $B_t = 1/b_t^2$. By comparing the results of both formulations, the numerical stability and effectiveness of a particular numerical technique can be checked. Furthermore, two completely different optimization techniques are employed and the results are compared for the same reason. The first is a direct formulation of the problem expressed in equation (10), and the second is a nonlinear programming technique called the flexible tolerance method (Himmelblau, 1972). In what follows, these methods are presented for the second formulation only (i.e., equation (11)).

Direct Method. The minimum of the function $\Phi(\alpha_t, \beta_t, \gamma_t, A_t, B_t)$ occurs when

$$\left.\begin{aligned} \frac{\partial\Phi}{\partial\mu} &= \sum_1^n 2\epsilon_i \{A_t(r_{11}x_f^i + r_{21}y_f^i + r_{31}z_f^i)\left(\frac{\partial r_{11}}{\partial\mu}x_f^i + \frac{\partial r_{21}}{\partial\mu}y_f^i + \frac{\partial r_{31}}{\partial\mu}z_f^i\right) \\ &\quad + B_t(r_{12}x_f^i + r_{22}y_f^i + r_{32}z_f^i)\left(\frac{\partial r_{12}}{\partial\mu}x_f^i + \frac{\partial r_{22}}{\partial\mu}y_f^i + \frac{\partial r_{32}}{\partial\mu}z_f^i\right) \\ &\quad - (r_{13}x_f^i + r_{23}y_f^i + r_{33}z_f^i)\left(\frac{\partial r_{13}}{\partial\mu}x_f^i + \frac{\partial r_{23}}{\partial\mu}y_f^i + \frac{\partial r_{33}}{\partial\mu}z_f^i\right) = 0 \\ &\qquad \mu \Rightarrow \alpha_t, \beta_t, \gamma_t \\ \frac{\partial\Phi}{\partial A_t} &= \sum_1^n \epsilon_i(r_{11}x_f^i + r_{21}y_f^i + r_{31}z_f^i) = 0 \\ \frac{\partial\Phi}{\partial B_t} &= \sum_1^n \epsilon_i(r_{12}x_f^i + r_{22}y_f^i + r_{32}z_f^i) = 0 \end{aligned}\right\} \tag{12}$$

The equations (12), together with expression for ϵ_i (equation (11)), constitute five highly nonlinear, strongly coupled algebraic equations to be solved for the unknowns α_t, β_t, γ_t, A_t, and B_t. An IMSL library routine called ZSCNT is employed for the solution of a system of nonlinear equations. This routine requires initial guesses to be supplied by the user.

Flexible Tolerance Method. This is a direct search method which, in general, can accommodate any nonlinear equality and/or inequality constraints, and does not need derivatives to be supplied. An initial tolerance criterion as well as initial guesses are required to initiate the search. The method is explained in detail and a fortran code is provided by Himmelblau (1972). This fortran code was modified to suit the complier of the VAX-11 computer available, and was tested with several optimization problems of known solutions. The present problem was then solved by introducing the following inequality constraints:

$$A_t, B_t \geq 0, \quad 0 \leq \alpha_t, \beta_t, \gamma_t \leq 2\pi \tag{13}$$

Comparison of Methods of Cone Fitting and Results. The cone optimization problem was solved for both formulation with both methods. It may be surmised that both formulations should naturally give the same results. However, during test runs it was discovered that this is so for a reasonably behaving set of unit vectors. In the case where unit vectors do not describe approximately a conical surface, e.g., if they all lie on a single plane, two formulations were found to give completely different results for the flexible tolerance method, and to fail to give a solution in the case of the direct method. Failure to get the same results from both formulations therefore indicates an ill-conditioned problem giving rise to numerical instabilities. An exhaustive search was made to identify any local minimum or saddle point by trying several sets of initial guesses. Some of the results that are believed to be representative of the effectiveness of the two methods are given in Table 1. In the first two rows of the table different results are obtained for the same initial guesses from the two methods with formulation I of equation (8). Although α_t and β_t parameters defining the orientation of the cone axis are almost the same, the apex angles are quite different, the flexible tolerance method yielding an elliptical cone and the direct method a circular one. To see which solution is the correct one, the results obtained from the direct method are supplied as initial guesses for the flexible tolerance as shown in row 3 of Table 1, and the results of the flexible tolerance method are given as initial guesses for the direct method in row 4. It can be seen from the table that both methods now give the results obtained initially from the flexible tolerance, i.e., those of row 1. This indicates that the direct method results are not reliable and dependent upon initial guesses. To see if this behavior is due to numerical instabilities or an inherent feature of the direct method, in row 5 we gave the results of row 2 as initial guesses for the direct method with formulation II of equation (11). Since the results of rows 5 and 2 are the same, there are no numerical instabilities involved, thus indicating that the direct method leads to a local minimum or possibly to a saddle point unless initial guesses are reasonably close to the global minimum. This is further verified by the test of row 6 where the results of row 4, i.e., correct solution (global minimum) are supplied as initial guesses to the direct method again with formulation II, yielding the same correct solution. In row 7, the flexible tolerance method is checked with formulation II by using the same initial guesses of row 1, yielding the same results. Finally, it should be noted that the flexible tolerance method locates the global minimum no matter how far the initial guesses are from the solution, as can be observed from rows 1 and 7. All these results indicate that the flexible

Downloaded From: https://biomechanical.asmedigitalcollection.asme.org on 06/29/2019 Terms of Use: http://www.asme.org/about-asme/terms-of-use

Table 1 Comparison of cone optimization methods

(Apex angles: $\eta_t = \tan^{-1} a_t$ or $\tan^{-1}\sqrt{1/A_t}$; $\zeta_t = \tan^{-1} b_t$ or $\tan^{-1}\sqrt{1/B_t}$)

Test No.	Method	Formulation I: equation (8) II: equation (11)	Initial Guesses a_t or A_t, b_t or B_t α_t, β_t, γ_t (radians)	Results a_t or A_t, b_t or B_t α_t, β_t, γ_t (radians)	Apex angles $2\eta_t$ $2\zeta_t$
1	Flexible tolerance	I	$a_t = 0.7$, $b_t = 0.7$ -1.57, 0.0, 0.0	$a_t = 3.37$, $b_t = 8.65$ -1.54, 0.59, 1.74	147 deg 168 deg
2	Direct method	I	$a_t = 0.7$, $b_t = 0.7$ -1.57, 0.0, 0.0	$a_t = 4.40$, $b_t = 4.40$ -1.55, 0.61, 0.88	154 deg 154 deg
3	Flexible tolerance	I	$a_t = 4.40$, $b_t = 4.40$ -1.55, 0.61, 0.88	$a_t = 3.37$, $b_t = 8.65$ -1.54, 0.59, 1.74	147 deg 168 deg
4	Direct method	I	$a_t = 3.37$, $b_t = 8.65$ -1.54, 0.59, 1.74	$a_t = 3.37$, $b_t = 8.64$ -1.54, 0.59, 1.74	147 deg 168 deg
5	Direct method	II	$A_t = 0.052$, $B_t = 0.052$ -1.55, 0.61, 0.88	$A_t = 0.052$, $B_t = 0.052$ -1.55, 0.61, 0.1	154 deg 154 deg
6	Direct method	II	$A_t = 0.088$, $B_t = 0.013$ -1.54, 0.59, 1.74	$A_t = 0.088$, $B_t = 0.013$ -1.54, 0.59, 1.74	147 deg 168 deg
7	Flexible tolerance	II	$A_t = 2.04$, $B_t = 2.04$ -1.57, 0.0, 0.0	$A_t = 0.088$, $B_t = 0.013$ -1.55, 0.59, 1.74	147 deg 168 deg

tolerance method is much more reliable than the direct method. It should, however, be pointed out that the direct method is much faster in execution than the flexible tolerance method.

In view of the foregoing discussion along with the results presented in Table 1, the following values can confidently be quoted as the desired composite sinus cone parameters.

Cone size (apex angles): $\eta_t = 147$ deg, $\zeta_t = 168$ deg
Orientation of the cone: $\alpha_t = -88$ deg, $\beta_t = 34$ deg, $\gamma_t = 100$ deg

The above results were obtained by utilizing 32 equally spaced data points on the $\bar{\theta} = \bar{\theta}(\phi)$ curve of Fig. 5. as can be seen from Fig. 5, $\bar{\theta} = \bar{\theta}(\phi)$ curve shows steep slopes in some regions, suggesting inclusion of additional data points in these regions. In fact, the data points were increased from 32 to 48 and cone parameters were reevaluated. With this extended data set the orientation of the cone remained unchanged, and apex angles changed no more than 2 degrees (148 deg, 170 deg).

The resulting Euler angles given above for the orientation of the cone can be better interpreted either by means of projected angles on the cardinal planes, or spherical angles measured with respect to the anatomical directions. The axis of the composite sinus cone makes 1.5 deg with the lateral direction and 88.5 deg with the inferior direction in the frontal plane ($y_0 z_0$), and makes 33.8 deg with the lateral direction and 56.2 deg with the anterior direction in the transverse plane ($x_0 y_0$). The major axis of the cone, which corresponds to 170 deg apex angle, makes 10 deg with the anterior direction, and 80 deg with the superior direction in the sagittal plane ($x_0 z_0$). In terms of the spherical angles with respect to the anatomical directions, cone axis makes 56.2, 33.8, and 88.8 deg with respect to x_0, y_0, and z_0 axes of the torso-fixed system, respectively. The major axis of the cone cross section makes 35.0, 57.1, and 79.5 deg, whereas the minor axis makes 82.0, 83.0, and 10.6 deg with respect to the aforementioned anatomical directions x_0, y_0, and z_0, respectively.

Concluding Remarks

In this paper a three-dimensional kinematic model of the human shoulder complex has been proposed by utilizing the concepts of kinematic links as well as joint sinuses. By assigning appropriate coordinate systems, parameters required for complete quantitative description of the proposed model have been identified. In order to determine the values of these parameters, available statistical data base for the shoulder complex has been cast in a form compatible with the model, i.e., a set of unit vectors describing the circumductory motion of the upper arm. This set of unit vectors has been employed in determining the parameters of a composite shoulder complex sinus of a simplified version of the proposal model. Two methods, namely the flexible tolerance and direct methods, have been formulated and tested for the determination of the elliptical cone describing the composite sinus. Various salient features of the two methods have been discussed, and interpretation of the results have been presented.

The mathematical modelling and its solution for the initially proposed more comprehensive kinematic model will be dealt with in Part II of this paper.

References

Dempster, W. T., 1965, "Mechanisms of Shoulder Movement," *Archives of Physical Medicine and Rehabilitation*, Vol. 46, No. 1-A, pp. 49-69.

Dvir, Z., and Berme, N., 1978, "The Shoulder Complex in Elevation of the Arm: A Mechanism Approach," *Journal of Biomechanics*, Vol. 11, No. 5, pp. 219-225.

Engin, A. E., 1980, "On the Biomechanics of the Shoulder Complex," *Journal of Biomechanics*, Vol. 13, No. 7, pp. 575-590.

Engin, A. E., Peindl, R. D., Berme, N., and Kaleps, I., 1984, "Kinematic and Force Data Collection in Biomechanics by Means of Sonic Emitters-I: Kinematic Data Collection Methodology," ASME JOURNAL OF BIOMECHANICAL ENGINEERING, Vol. 106, pp. 204-211.

Engin, A. E., and Peindl, R. D., 1985, "Passive Resistive and Damping Properties of Human Shoulder Complex," *AFAMRL Report*, AFAMRL-TR-84-051.

Engin, A. E., and Chen, S. M., 1986a, "Statistical Data Base for the Biomechanical Properties of Human Shoulder Complex-I: Kinematics of the Shoulder Complex," ASME JOURNAL OF BIOMECHANICAL ENGINEERING, Vol. 108, pp. 215-221.

Engin, A. E., and Chen, S. M., 1986b, "Statistical Data Base for the Biomechanical Properties of Human Shoulder Complex-II: Passive Resistive Properties Beyond the Shoulder Complex Sinus," ASME JOURNAL OF BIOMECHANICAL ENGINEERING, Vol. 108, pp. 222-227.

Engin, A. E., and Tümer, S. T., 1987, "Çok Sayıda Ses Kaynağı Yardımıyla Hareket Analizi-II: Hata Analizi ve Bir Uygulama," *Makina Tasarim ve İmalat Dergisi*, Vol. 1, No. 4, pp. 181-186.

Gray's Anotomy, 1973, 35th British Edition (edited by Warwick, R., and Williams, P. L.), W. B. Saunders, Philadelphia.

Himmelblau, D. M., 1972, *Applied Nonlinear Programming*, McGraw-Hill Inc., N.Y.

Högfors, C., Sigholm, G., and Herberts, P., 1987, "Biomechanical Model of the Human Shoulder-I: Elements," *Journal of Biomechanics*, Vol. 20, No. 2, pp. 157-166.

Steindler, A., 1955, *Kinesiology of the Human Body*, Thomas, Springfield, Ill.

Downloaded From: https://biomechanical.asmedigitalcollection.asme.org on 06/29/2019 Terms of Use: http://www.asme.org/about-asme/terms-of-use